Research article

LUMINESCENCE
The Journal of Biological and Chemical Luminescence

Received: 27 July 2015, Revised: 13 November 2015, Accepted: 26 December 2015 Published online in Wiley Online Library: 3 February 2016

(wileyonlinelibrary.com) DOI 10.1002/bio.3101

Study of photoluminescence characteristics of CdSe quantum dots hybridized with Cu nanowires

Xiaochun Chi,[a] Yinghui Wang,[a]* Jiechao Gao,[a] Qinghui Liu,[a] Ning Sui,[a] Jinyang Zhu,[a] XueCong Li,[b] Haigui Yang,[c] Lu Zou,[a] Jun Kou[d] and Hanzhuang Zhang[a]*

ABSTRACT: The photoluminescence (PL) characteristics of semiconductor CdSe quantum dots (QDs) aggregated on Cu nanowires (NWs) were studied in detail. The PL relaxation dynamic data show that Cu NWs improve the PL intensity of CdSe QDs by accelerating the emission relaxation rate. The temperature-dependent PL data and excitation intensity-dependent PL data suggest that the activation energy of CdSe QDs might decrease due to the excellent heat transfer properties and the plasmon effect of Cu NWs. Copyright © 2016 John Wiley & Sons, Ltd.

Keywords: photoluminescence; quantum dots; Cu nanowires; plasmon effect

Introduction

Heavy metal materials with a nanostructure show a localized surface plasmon resonance (LSPR) effect that reflects the collective oscillation behavior of electrons on the surface of the metal (1,2). The LSPR spectral property is dependent on the size and shape of the metal nanostructure, the dielectric constant, the sounding environment and the size distribution (3,4). Cu nanowires (Cu NWs) are a complex type of novel heavy metal nano-material (5) and have huge potential in the fields of photonics and biosensing due to their interesting physical properties (6,7). According to previous reports (8,9), the photoluminescence (PL) characteristics of light-emitting materials hybridized with a metal nanostructure are improved through coherent coupling, showing that the photophysical features of light-emitting materials could be manipulated by the electric field originating from the LSPR. This implies that Cu NWs may have the potential to improve the PL of light-emitting materials, which could then be applied in optoelectronic research. Semiconductor quantum dots (QDs) have many excellent properties (10) and can be used in optoelectronic devices (11), biomedical imaging (12), etc. CdSe QDs are traditional semiconductor QDs (13,14) that can be used as a model to clarify the PL characteristics manipulated by Cu NWs.

In this study, CdSe QDs were attached to the surface of a network based on Cu NWs (CdSe QDs/Cu NWs). Because of the contribution from Cu NWs, the PL intensity of CdSe QDs/Cu NWs enhanced mechanism. In order to clarify the mechanism behind the improvement, the PL characteristics of CdSe QDs/Cu NWs were investigated in detail.

Experimental

CdSe QDs and the Cu NWs were purchased from Nanjing XFNANO Materials Tech Co., Ltd. (Nanjing, China) Sixty microliters of Cu NW solution was spun coated onto a glass plate using a spin coater (KW-4A) to form a homogeneous Cu NW network after the ethanol solvent had been volatilized. Then, 40 μL of CdSe QDs solution was impregnated into the Cu NW network and a normal quartz plate, respectively. In particular, poly(vinyl alcohol) solution was spun coated onto the Cu NW network, to avoid oxidation of the Cu NWs. In this way, hybrid CdSe QDs/Cu NWs (#1) and pure CdSe QDs (#2) were prepared.

Steady-state absorption measurements were carried out using a UV–Vis spectrophotometer (TU-1810PC, Purkinje, Beijing, China). The PL spectra were recorded using a fiber optic spectrometer (Ocean Optics, USB4000, Beijing, China) at an excitation of 400 nm. Time-correlated single photon counting was performed using a fluorescence spectrometer (mini-τ, Edinburgh Photonics, Beijing, China) (15). The surface morphology of the Cu NWs and hybrid CdSe QDs/Cu NWs was investigated using a field emission transmission electron microscope (JEOL JEM-2100F, Beijing, China).

Results and discussion

Figure 1(A) and (B) are TEM image of Cu NWs and hybrid CdSe QDs/Cu NWs, respectively. The size of the CdSe QDs was ~ 3 nm.

* Correspondence to: Yinghui Wang, Hanzhuang Zhang, Key Laboratory of Physics and Technology for Advanced Batteries (Ministry of Education), College of Physics, Jilin University, Changchun 130012, China. E-mail: yinghui_wang@jlu.edu.cn; zhanghz@jlu.edu.cn

[a] Key Laboratory of Physics and Technology for Advanced Batteries (Ministry of Education), College of Physics, Jilin University, Changchun 130012, China

[b] Department of Physics, Tianjin Polytechnic University, Tianjin 300387, China

[c] Key Laboratory of Optical System Advanced Manufacturing Technology, Changchun Institute of Optics, Fine Mechanics and Physics, Chinese Academy of Sciences, Changchun 130033, China

[d] Beijing Institude of Aerospace Control Devices, Beijing 100000, China

LUMINESCENCE
The Journal of Biological and Chemical Luminescence

The length of the Cu NWs was ~ 5 μm (not shown) and the diameter was ~ 50 nm, as seen in Fig. 1(A). Cu NWs have a large surface area that could effectively absorb a large number of CdSe QDs. As seen in Fig. 1(B), many CdSe QDs aggregated on the surface of the Cu NWs and the thickness of the CdSe QDs on Cu NWs is ~ 10 nm. Cu NWs and CdSe QDs have different refractive indexes, and a LPRS effect occurred in the hybrid system when it was excited by light. Figure 1(C) shows the UV–Vis absorption and PL spectra of the CdSe QDs in solution. The absorption maximum of the CdSe QDs is located at ~ 518 nm and the corresponding PL peak is at ~ 545 nm.

Figure 2(A) gives the PL spectra of #1 and #2, which show that the intensity of the former is about twice that of the latter. Meanwhile, the PL peak of #1 is almost the same as that of #2. The enhancement of the PL intensity could be attributed to the LPRS effect (16) and light scattering originating from Cu NWs. The PL peak of CdSe QDs does not vary because CdSe QDs aggregated both inside and outside the Cu NWs. Because the PL spectrum of #1 is similar to that of #2, it was not possible to determine whether the PL characteristics of QDs are coupled with plasmon originating from Cu NWs. The time-dependent PL decay curves of #1 and #2 are presented in Fig. 2(B), to determine the role of the LPRS effect on the PL characteristics of CdSe QDs. It is apparent that both #1 and #2 show non-exponential relaxation behavior following photoexcitation. The relaxation rate for #1 is faster than that for #2 because of the energy transfer effect on LSPR coupling between the Cu NWs and QDs (17). Therefore, an increase in the radiative relaxation rate may be responsible for enhancement of the PL in CdSe QDs. To further clarify the role of LPRS in the PL dynamics, PL decay traces are fitted with a continuous distribution function of decay rates (18):

$$I(t) = I(0)\int_{\gamma=0}^{\infty}\varphi(\gamma)\exp(-\gamma t)d\gamma \quad (1)$$

where $\varphi(\gamma)$ is a distribution of decay rates with the dimension of time; $I(t)$ is the fluorescence intensity; $\varphi(\gamma)$ describes a distribution of the concentration of emitters with a certain γ, weighted by the corresponding γ_{rad} (19). $\varphi(\gamma)$ is the log-normal distribution function, as described below:

$$\varphi(\gamma) = A\exp\left[\frac{-\ln^2(\gamma/\gamma_{MF})}{w^2}\right] \quad (2)$$

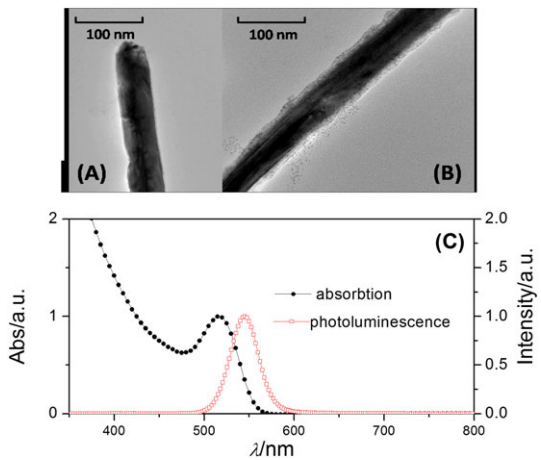

Figure 1. TEM image of (A) Cu NWs, and (B) hybrid CdSe QDs/Cu NW; (C) absorption and PL spectra of CdSe QDs in solution.

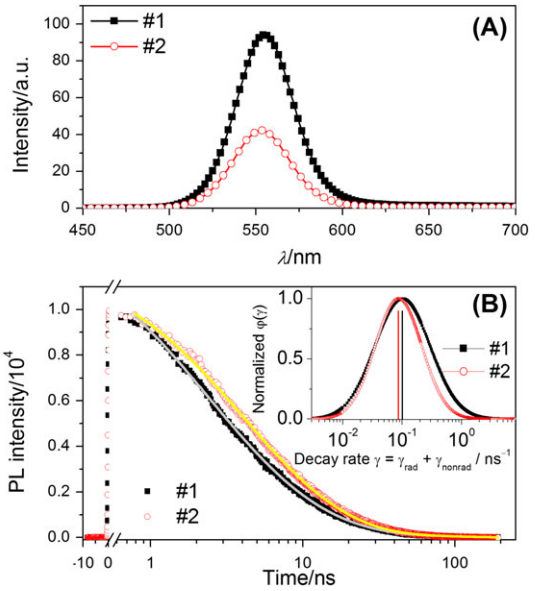

Figure 2. (A) PL spectra of #1 and #2; (B) corresponding time-resolved PL decay curves detected at 550 nm. (Inset) Their corresponding decay-rate distributions $\varphi(\gamma)$. γMF of #1 and #2 are 0.101 and 0.087 ns^{-1}, respectively, and the widths ($\Delta\gamma$) of their distribution function are 0.439 and 0.288 ns^{-1}, respectively.

where γ_{MF} is the most-frequency decay rate corresponding to the maximum of $\varphi(t)$; w is a dimensionless width parameter that determines the distribution width ($\Delta\gamma$) at $1/e$; A is the normalization constant, so that $\int\varphi(\gamma)d\gamma = 1$. The fitted lines are shown in Fig. 2(B) with solid lines, and the corresponding rate distribution functions are summarized in the inset to Fig. 2(B). The fitted results show that γ_{MF} is 0.101 and 0.087 ns^{-1} for #1 and #2, respectively. The distribution width could be calculated as:

$$\Delta\gamma = 2\gamma_{MF}\sinh w \quad (3)$$

As seen in the inset to Fig. 2(B), $\Delta\gamma$ is 0.439 and 0.288 ns^{-1} for #1 and #2, respectively, and the rate distribution width becomes broader under the manipulation of plasmon resonance effect. This indicates that the relaxation behavior of #1 is complex in comparison with that of #2. The relaxation rate for #1 is faster than that for #2, which explains the enhancement in the PL intensity. Moreover, the variance in the relaxation rate might be attributed to manipulation of the LSPR effect originating from Cu NWs.

The temperature-dependent PL intensities of #1 and #2 excited using a continuum laser with a wavelength of 400 nm are presented in Fig. 3(A), which shows that the PL intensity gradually decreases with increasing temperature. According to a previous report (20), this non-radiative relaxation indicates a thermal escape from the QDs, assisted by photon-electron coupling with the scattering of longitudinalo optical (LO) phonons. The data in Fig. 3(A) are modeled using the equation:

$$I(T) = I_0\left[1 + C\exp\left(-\frac{E_a}{k_B T}\right)\right]^{-1} \quad (4)$$

and the results are shown as solid lines. The activation energy, E_a, is 177 and 210 meV for #1 and #2, respectively. This indicates that Cu NWs could decrease the activation energy of CdSe QDs and facilitate thermal exchange between the CdSe QDs and the

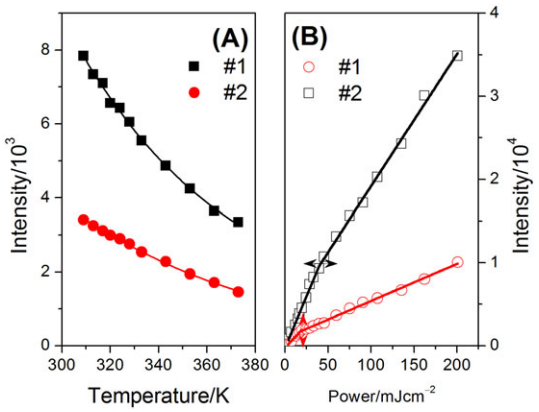

Figure 3. PL spectra of #1 and #2; (B) excitation intensity-dependent integrated PL intensity of #1 and #2.

surrounding environment. Apparently, the LSPR might play an important role in changing the activation energy of QDs, which is consistent with a previous report (21).

In order to further investigate the role of LSPR originating from Cu NWs on the PL characteristics of CdSe QDs, the excitation intensity-dependent integrated photoluminescence intensities (IPLI) of #1 and #2 at room temperature were compared (Fig. 3B), and all the PL spectra of CdSe QDs were excited using a continuum laser with wavelength of 400 nm. When the excitation intensity is lower than ~ 20 mJ/cm^2, the IPLI values of both #1 and #2 are linearly enhanced with the excitation intensity. The ratio of the slope between #1 and #2 is ~ 2.3, which is similar to the results shown in Fig. 2(A). In this situation, the thermal accumulation effect on the interacting samples originating from the continuum laser could be ignored. After this, a turning point appears in the enhancement of PL intensity, as the excitation intensity increase to 50 mJ/cm^2 for #1 and 21 mJ/cm^2 for #2. This indicates that the thermal accumulation effect cannot be ignored at high excitation intensities. The threshold for #1 is higher than that for #2, which could be assigned to the excellent heat transfer characteristics of Cu NWs. In addition, it is interesting that the ratio of slope between #1 and #2 is ~ 3.5 when the excitation intensity increases towards the excitation intensity threshold, suggesting that the IPLI of #1 is approximately three times higher than that of #2, when the thermal accumulation effect affects the PL characteristics of CdSe QDs. This situation might also be attributed to the contribution made by of the excellent heat transfer characteristics and the LPRS effect of Cu NWs, which effectively transfer heat from CdSe QDs to the environment, under the interaction of the continuous laser. It is reasonable to consider that the heat transfer properties of Cu NWs might also influence the change in the activation energy of QDs, because it is helpful for heat to transfer from the environment of QDs. Therefore, it is reasonable to expect that the LSPR effect and the heat transfer property of Cu NWs might be responsible for the improvement in the PL characteristics of CdSe QDs.

Conclusions

The PL characteristics of CdSe QDs inside and outside a Cu NWs network are compared in detail. The PL data show that Cu NWs improve the PL intensity of CdSe QDs by increasing the emission relaxation rate, which is attributed to the LPRS effect. Meanwhile, Cu NWs facilitate the exchange of heat between CdSe QDs and the environment, decreasing the activation energy due to their rapid heat transferring ability and the plasmon effect, which might be useful in the application of CdSe QDs at high temperatures.

Acknowledgements

This work was supported by the National Natural Science Foundation of China (Nos. 11474131, 21103161, 11274142 11204011, 11304007 and 11304058), National Found for Fostering Talents of basic Science (NO. J1103202), State Key Laboratory of Luminescence and Applications (SKLLA201303), the China Postdoctoral Science Foundation (2011M500927 and 2013T60319) and Science & Technology Development Foundation of Tianjin higher education institutions (No. 20140904).

References

1. He L, Musick MD, Nicewarner SR, Salinas FG, Benkovic SJ, Natan MJ, et al. Label-free potentiometry for detecting DNA hybridization using peptide nucleic acid and DNA probes. J Am Chem Soc 2000;122:9071–7.
2. Haes AJ, van Duyne RP. A nanoscale optical biosensor: sensitivity and selectivity of an approach based on the localized surface plasmon resonance spectroscopy of triangular silver nanoparticles. J Am Chem Soc 2002;124:10596–640.
3. El-Brolossy TA, Abdallah T, Mohamed MB, Abdallah S, Easawi K, Negm S, et al. Shape and size dependence of the surface plasmon resonance of gold nanoparticles studied by photoacoustic technique. Phys J-Spec Top 2008;153:361–4.
4. Westcott SL, Jackson JB, Radloff C, Halas NJ. Relative contributions to the plasmon line shape of metal nanoshells. Phys Rev B 2002;66:15543–5.
5. Zhang DQ, Wang RR, Wen WC, Weng D, Cui X, Sun J, et al. Synthesis of ultralong copper nanowires for high-performance transparent electrodes. J Am Chem Soc 2012;134:14283–6.
6. Kim SS, Na SI, Jo J, Kim DY, Nah YC. Plasmon enhanced performance of organic solar cells using electrodeposited Ag nanoparticles. Appl Phys Lett 2008;93:073307–3.
7. Choulis SA, Mathai MK, Choong VE. Influence of metallic nanoparticles on the performance of organic electrophosphorescence devices. Appl Phys Lett 2006;88:213503–3.
8. Huang HW, Huang SW, Yuan SS, Qu CT, Chen Y, Xu ZJ, et al. High-sensitivity biosensors fabricated by tailoring the localized surface plasmon resonance property of core–shell gold nanorods. Anal Chim Acta 2011;683:242–72.
9. Dinh TV, Cullum BM, Stokes DL. Nanosensors and biochips: frontiers in biomolecular diagnostics. Sensor Actuat B-Chem 2001;74:2–11.
10. Yoffe D Semiconductor quantum dots and related systems: electronic, optical, luminescence and related properties of low dimensional systems. Adv Phys 2001;50:1–208.
11. Sun QJ, Wang YA, Li LS, Wang DY, Zhu T, Xu J, et al. Bright, multicoloured light-emitting diodes based on quantum dots. Nature 2007;1:717–22.
12. Lim YT, Kim S, Nakayama A, Stott NE, Bawendi MG, Frangioni JV. Selection of quantum dot wavelengths for biomedical assays and imaging. Mol Imaging 2003;2:50–64.
13. Surana K, Singh PK, Rhee HW, Bhattacharya B. Synthesis, characterization and application of CdSe quantum dots. J Ind Eng Chem 2014;20:4188–93.
14. Rosetti R, Brus L. Electron-hole recombination emission as a probe of surface chemistry in aqueous cadmium sulfide colloid. J Phys Chem 1982;86:4470–2.
15. Sui N, Zou L, Song YF, Zhong QL, Wang YH, Wei XP, et al. Pi-conjugated unit-dependent optical properties of linear conjugated oligomers. Chin J Chem Phys 2014;27:315–20.
16. Brolo AG, Kwok SC, Moffitt MG, Gordon R, Riordon J, Kavanagh KL. Enhanced fluorescence from arrays of nanoholes in a gold film. J Am Chem Soc 2005;127:14936–41.
17. Lee YB, Lee SH, Lee S, Lee H, Kim JY, Joo J. Surface enhanced Raman scattering effect of CdSe/ZnS quantum dots hybridized with Au nanowire. Appl Phys Lett 2013;102:033109.

LUMINESCENCE
The Journal of Biological and Chemical Luminescence

18. Nikolaev AS, Lodahl P, van Driel AF, Koenderink AF, Vos WL. Strongly nonexponential time-resolved fluorescence of quantum-dot ensembles in three-dimensional photonic crystals. Phys Rev B 2007;75:115302–5.
19. van Driel AF, Nikolaev IS, Vergeer P, Lodahl P, Vanmakekelbergh D, Vos WL. Statistical analysis of time-resolved emission from ensembles of semiconductor quantum dots: interpretation of exponential decay models. Phys Rev B 2007;75:35329–8.
20. Valerini D, Creti A, Lomascolo M, Manna L, Cingolani R, Anni M. Temperature dependence of the photoluminescence properties of colloidal CdSeZnS core/shell quantum dots embedded in a polystyrene matrix. Phys Rev B 2005;71:235409–6.
21. Qian C, Xu EZ, Sui N, Wang YH, Wu HL, Song YF, et al. Studying of the photoluminescence of MEH–PPV–Au nanoparticles hybrid system. J Mod Opt 2015;62:387–91.

